International Journal of Enhanced Research in Science Technology & Engineering, ISSN: 2319-7463
Vol. 3 Issue 7, July-2014, pp: (240-250), Impact Factor: 1.252, Available online at: www.erpublications.com

Numerical study of heat and mass transfer in liquid film evaporation by a porous layer within a vertical flow channel

Lahcen Bellouch[1], Youness EL Hammami[2], Larbi Khalal[3], Rachid Mir[4], Touria Mediouni[5]

[2,4,5]Professor, Mechanics, Process of Energy and Environment Laboratory, IbnZohr University, ENSA, Morocco
[1,3]PHD student, Mechanics, Process of Energy and Environment Laboratory, IbnZohr University, ENSA, Morocco

Abstract: The purpose of this study is to analyses the combined heat and mass transfer of liquid film evaporation by covering a porous layer of left plate within a vertical channel. Since the theoretical analyses of the liquid film evaporation problem is complicated due to transport phenomena involve coupled heat and mass transfer at the saturated porous layer within a vertical channel, the liquid and air streams are modeled as two coupled laminar boundary layers incorporating non-Darcian models of the inertia and boundary effects.
The governing equations for the liquid flow film and gas stream coupled through the interface with the appropriate boundary conditions are solved numerically by using a finite difference method. Each system of the finite-difference equations forms a tridiagonal matrix equation which can be solved by the Thomas algorithm. The aims of this paper are to improve our understanding by examining the effects of porosity, Reynolds number and humidity on the heat and mass transfer performance in the evaporation of liquid film. The results of simulation show the importance of porosity, Reynolds number and humidity to enhance heat and mass transfer performance across the liquid-film interface. The comparisons of interfacial temperature and dimensionless interfacial mass concentration with the literature results are in good agreement.

Keywords: Liquid film evaporation; Porous layer; Heat and mass transfer; vertical channel.

Introduction

The liquid film evaporation with combined heat and mass transfer is of importance in many industrial processes such as evaporative cooling for waste heat disposal, evaporative fluid coolers, turbine blade cooling, combustion premixing and the distillation of a volatile component from a mixture with in volatiles. The previous studies are generally related to the liquid film evaporation along a vertical duel. In vertical heated channel, Feddaoui et al. [1, 2] examined the effect of combined thermal and solutal buoyancy forces on laminar mixed convection heat and mass transfer with film evaporation in both symmetrically and asymmetrically heated vertical channel.

As far as heat and mass transfer in porous medium is concerned, Rees and Vafai [3] investigate the free convection boundary layer flow of a Darcy-Brinkman fluid induced by a horizontal surface embedded in a fluid -saturated porous layer. Later Alazmi and Vafai [4] analysed in detail the fluid flow and heat transfer with interfacial conditions between a porous medium and a fluid layer. Chou and his colleagues studied numerically the evaporation along a vertical plate covered with a thin porous layer (Leu et al. [5]) and along a saturated porous layer inside an inclined flow channel (Chou et al. [6]). On the other hand (Jin-Sheng et al. [7]) are analyzed the forced convection liquid film evaporation problem in a saturated non-Darcian porous medium. This model including inertia, boundary and convective effects is employed to represent the momentum transport of these two streams. El Hammami et al. [8, 9] are analysed two cases; the first one treated the combined heat and mass transfer of liquid film evaporation by covering a porous layer of left plate within an inclined channel. A marching procedure is employed for solution of the respective goveming equations for the liquid film and air stream together in corporate with non-Darcian Models. The results of simulation show the importance of porosity and thickness porous layer to enhance heat and mass transfer performance across the liquid-film interface, the second one presents a numerical study of heat transfer and mass during the condensation of a laminar film water vapor in an inclined porous channel wall. In the porous medium, the flow is described by the Darcy-Brinkman model-Forchheimer.

Recently, Halder et al. [10] they tried to solve a conjugate problem of microwave heating, containing both the porous material and the outside environment, and to discuss and quantify the factors on which the heat and mass transfer coefficients at the porous media surface depends. Touati et al. [11] which have suggested to studying the coupling of the equations of the air in the layer of interface with those which describe the transfer of heat and mass in the porous mediums permits to model the phenomena of the operation of drying without having recourses to the global coefficient of transfers of heat and mass between the air and the product.

The aims of this study is to improve our understanding and comparing the effects of porosity, Reynolds Number and Humidity on the heat and mass transfer performance by a vaporizing a liquid film of water in a saturated non-Darcian porous medium. The coupled conservation equations for both the moist-air and liquid film streams are solved together. The parametric studies on the effects of the inlet conditions and the porosity of the porous medium on the heat and mass performances of liquid film evaporation are examined in detail.

Analysis

A. Physical model and assumption.

The geometry of the problem concerns vertical parallels plates with channel height H and channel width W (Fig 1). The left plate of channel is covered by a porous layer and wetted by a falling liquid film flowing, and the right vertical plate is insulated. The liquid film is fed with an inlet liquid temperature T_{l0}, and inlet mass flow rate Γ_{L0}. The air-water vapour mixture enters the channel at temperature $T_0$and velocityu_0.

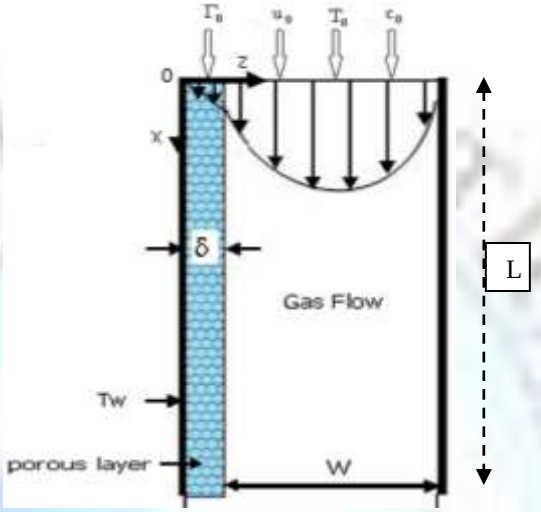

Figure 1. Physical Model

B. Mathematical Model

In the analysis, the following conventional assumptions are made:

- The flow is two dimensional and incompressible.
- The liquid saturated porous media is isotropic and homogeneous.
- The liquid and vapour phases are in local thermal equilibrium with the porous media.

On the above assumptions, the set of governing equations for the liquid film and air stream region are given as follows:

1) Basic equations for the liquid film.

The laminar liquid film flow and steady 2-D boundary layer equations for liquid film flow in porous medium. Adopting non-Darcien models and neglecting the transverse velocity component, the axial momentum and energy boundary layer equations can be further simplified as:

$$\left(\frac{\mu_L}{\varepsilon}\right)\frac{\partial^2 u_L}{\partial z^2} - \left(\frac{\mu_L}{K}\right)u_L - \left(\frac{\rho_L C}{\sqrt{K}}\right)u_L^2 + \rho_L g = 0 \quad (1)$$

$$u_L\left(\frac{\partial T_L}{\partial x}\right) = \alpha_e\left(\frac{\partial^2 T_L}{\partial z^2}\right) \quad (2)$$

Where K the permeability of the porous medium, *C* is the flow inertia parameter, ε is the porosity and α_e is the effective thermal diffusivity($\alpha_e = \frac{k_e}{\rho_L C_{p,L}}$). The effective thermal conductivity$k_e$is defined as$k_e = \varepsilon k_{liquid} + (1-\varepsilon)k_{solid}$.

The values for the permeability K and the inertia coefficient C in the momentum equations for the porous layer are given by Ergun [18] for packed beds of beads of diameter d_p and porosity ε.

$$K = \frac{d_p^2 \varepsilon^3}{175(1-\varepsilon)^2} \qquad \text{And} \qquad C = \left(\frac{1.75}{\sqrt{175}}\right)\varepsilon^{-\frac{1}{3}}\sqrt{K} \tag{3}$$

2) **Basic equations for gas flow**

The flow is considered to be two-dimensional; the regime is laminar and steady. Thus, the equations of continuity, momentum, energy and concentration can be written as:

$$\frac{\partial(\rho_G u_G)}{\partial x} + \frac{\partial(\rho_G u_G)}{\partial z} = 0 \tag{4}$$

$$\rho_G\left(\frac{u_G\,\partial u_G}{\partial x} + \frac{v_G\,\partial u_G}{\partial z}\right) = -\frac{dp}{dx} + \frac{\partial\left[\mu_G \frac{\partial u_G}{\partial z}\right]}{\partial z} + (\rho_G - \rho_0)g \tag{5}$$

$$\rho_G c_{pG}\left(\frac{u_G\,\partial T_G}{\partial x} + \frac{v_G\,\partial T_G}{\partial z}\right) = \frac{\partial\left[K_G \frac{\partial T_G}{\partial z}\right]}{\partial z} \tag{6}$$

$$\rho_G\left(\frac{u_G\,\partial c}{\partial x} + \frac{v_G\,\partial c}{\partial z}\right) = \frac{\partial\left[\rho_G D \frac{\partial c}{\partial z}\right]}{\partial z} \tag{7}$$

3) **Boundary and interfacial matching conditions.**

$$x = 0: \qquad u_G = u_0 \qquad T_G = T_0 \qquad c = c_0 \tag{8}$$

$$z = 0: \qquad u_L = v_L = 0 \qquad T_L = T_w \tag{9}$$

$$z = W + \delta: \qquad u_G = v_G = 0 \qquad \partial T_G/\partial z = 0 \qquad \partial c/\partial z = 0 \tag{10}$$

The solution from the liquid side and gas side satisfy the following interfacial matching conditions $(z = \delta)$:

- Continuities of velocity and temperature

$$u_I(x) = u_{G,I} = u_{L,I} \qquad T_I(x) = T_{G,I} = T_{L,I} \tag{11}$$

- Continuity of shear stress

$$\tau_I = \left[\mu \frac{\partial u}{\partial z}\right]_{L,I} = \left[\mu \frac{\partial u}{\partial z}\right]_{G,I}$$

(12)

4) **The transverse velocity component of the air-vapour mixture at the interface**

Is deduced by assuming the interface to be semi-permeable (Eckert and Drake, [12]). That is the solubility of air into the water is negligibly small, the velocity of the air-vapor mixture at the interface can be calculated by:

$$v_I = -D\frac{\frac{\partial c}{\partial z}}{(1-c_I)} \qquad (13)$$

The mass fraction at the interface w_I can be calculated using:

$$c_I = \frac{M_v p_{v,i}}{[M_a(p-p_{v,i})+M_v p_{v,i}]} \qquad (14)$$

Where p and $p_{v,i}$ are the total pressure and the vapor pressure at the interface, respectively. M_a and M_v are the molecular weights of air and vapor.

5) **Heat balance at the interface implying**

$$[-k\frac{\partial T}{\partial z}]_{L,I} = [-k\frac{\partial T}{\partial z}]_{G,I} + \dot{m}_I\gamma \qquad (15)$$

Where γ are the enthalpy of evaporation and $\dot{m}_I = \rho_G v_I$ the vaporgenerationrate.

The local heat exchange between the air stream and the liquid film depends on two related factors: the interfacial temperature gradient on the air side results in sensible convective heat transfer, and the evaporative mass transfer rate on the liquid film side results in latent heat transfer (Fedorov et al. [13]). The total convective heat transfer rate from the film interface to the air stream can be expressed as follows:

$$Q_t = Q_s + Q_L = [-k\frac{\partial T}{\partial z}]_{G,I} + \dot{m}_I\gamma \qquad (16)$$

For the purpose of generalizing the heat transfer results, the local Nusselt number along the interface gas-liquid is defined as:

$$Nu_x = \frac{h_T(2W)}{k_G} = \frac{Q_t(2W)}{k_G(T_I-T_b)} \qquad (17)$$

Basing the local mass-transfer coefficient on the diffusive mass flux, the local Sherwood number is defined as:

$$Sh_x = \frac{h_M(2W)}{D} = \dot{m}_I\frac{(1-c_I)(2W)}{\rho_G D(c_I-c_b)} \qquad (18)$$

Where the subscript b denotes the bulk quantities, the local bulk temperature T_b and mass fraction c_b in the channel are respectively defined as follows:

$$T_b = \frac{\int_\delta^W \rho_G c_{pG} u_G T dy}{\int_\delta^W \rho_G c_{pG} u_G dy} \quad \text{and} \quad c_b = \frac{\int_\delta^W \rho_G u_G c dy}{\int_\delta^W \rho_G u_G dy} \qquad (19)$$

At every axial location, the overall mass balance in the gas flow and liquid film should be satisfied:

$$W\rho_G u_0 = \int_\delta^W \rho_G u_G dy + \int_0^x \rho_G v_I T dx \qquad (20a)$$

$$\Gamma_0 = \int_0^{\delta} (\rho u dy)_L - \int_0^{x} \rho_G v_I dx \qquad (20b)$$

In the above formulation, the variations of the thermo-physical properties with temperature and air-vapour composition are included. They are calculated from the pure component data by means of mixing rules applicable to any multicomponent mixture. The pure component data are approximated by polynomials in term of temperature. For further details, the thermo-physical properties are available in (Fujii et al. [14] and Reid et al. [15]).

Numerical method and validation

In view of the impossibility of obtaining an analytic solution for the non-linear coupling differential equations, the conjugated problem defined by the parabolic systems, equation (1)-(7) with the appropriate boundary conditions are solved by a finite difference numerical scheme. The axial convection terms are approximated by the backward difference and the transversal convection and diffusion terms are approximated by the central difference. Each system of the finite-difference equations forms a tri-diagonal matrix equation which can be solved by the Thomas algorithm [16]. The correction of the pressure gradient and axial velocity profile at each axial station in order to satisfy the global mass flow constraint is achieved using a method proposed by Raithby and Schneider [17]. The equations are highly coupled and are solved iteratively at each downstream station until the overall mass conservation, equations (22) and the convergence of velocity; temperature and concentration are satisfied.

To obtain enhanced accuracy in the numerical computations, grids are chosen to be non-uniform in both axial and transverse directions. Accordingly the grids are compressed towards the interface gas-liquid and towards the entrance of channel. Grid-independence of the computation is tested and the corresponding results are presented in Table 1. It is noted that the differences shown in the temperature of the film at outlet and the density of the evaporation flux, using grids ranging from 51× (41+33) to 201× (161+99) were always less than 2 percent. In light of those results all further calculations were performed with the 101 × (81+66) grids.

The number of grid points in the transverse direction is noted N_L in the liquid film, $N_g$in the gas and $N_k$is the total grid points in the longitudinal direction.

Table 1: Influence of the gridwith $T_0 = T_{L0} = 25°C, P_0 = 1atm, T_w = 50°C, \varepsilon = 0.4, \phi = 80\%$ and W=0.05m

$N_k \times (N_g + N_L)$	Nu		Sh	
	Outlet Value	Error (%)	Outlet Value	Error (%)
51× (41+33)	43.340	2.00	2.450	1.96
101 × (41+33)	44.060	0.37	2.491	0.32
101 × (81+66)	44.163	0.14	2.496	0.12
201 × (81+66)	45.216	2.19	2.552	2.07
201× (161+99)	44.225	-	2.499	-

Validation of calculated

In fig. 2 the axial distributions of interfacial temperature and dimensionless interfacial mass concentration for various Re and ε are presented and compared with those of Chou et al. [6]. It is clear that generally the agreement between our prediction and study of Chou et al. [6]. Through this program test, the proposed numerical algorithm is considered to be suitable for the practical purpose.

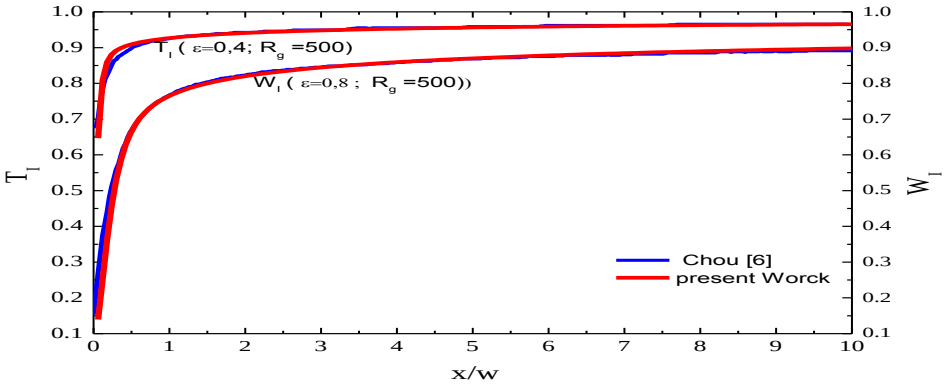

Figure 2. The axial distributions of interfacial temperature and dimensionless interfacial mass concentration for various Re and ε with δ=0.02, ϕ=70%

Results and Discussion

The present simulation has been performed by varying two parameters of the Reynolds number (Re ranging from 300 to 900) and relative humidity of air stream($\phi$is taken to be 40% and 80%), Also for a porous material parameters, porosityε(0.4 , 0.8). In respect to practical situation, certain conditions are selected: $T_0=T_{L0}=25°C$, $P_0=1atm$,Tw=50°C, L=0.5 m and W=0.05m

C. Influence of Reynolds number and porosity

The effects of introducing a liquid saturated porous material on the heat and mass transfer performance on the evaporation of liquid film flow within an air flow are analyzed. First we focused our study on the influence of air Reynolds number Re and the Porosity ε.

Fig.3 (a, b) shows the effects of the porosity and gas Reynolds numbers on the interfacial temperature and mass fraction. The curves in this figure indicate that the interfacial temperatures and mass fraction increases rapidly as the flow goes downstream up to the value x/w=2, but after this value they remains constant.

As expected, if the value of gas Reynolds number decreases more the values of T_I and W_I increase, it is also found that the value of the interfacial temperatures and mass fraction reduces as the porosity increases. This causes that the temperature of liquid-air interface increases in the presence of the porous layer saturated. This is due to the fact that the porous layer increases the heat exchange surface of the liquid film and thus favors the transfer of heat in the liquid film.

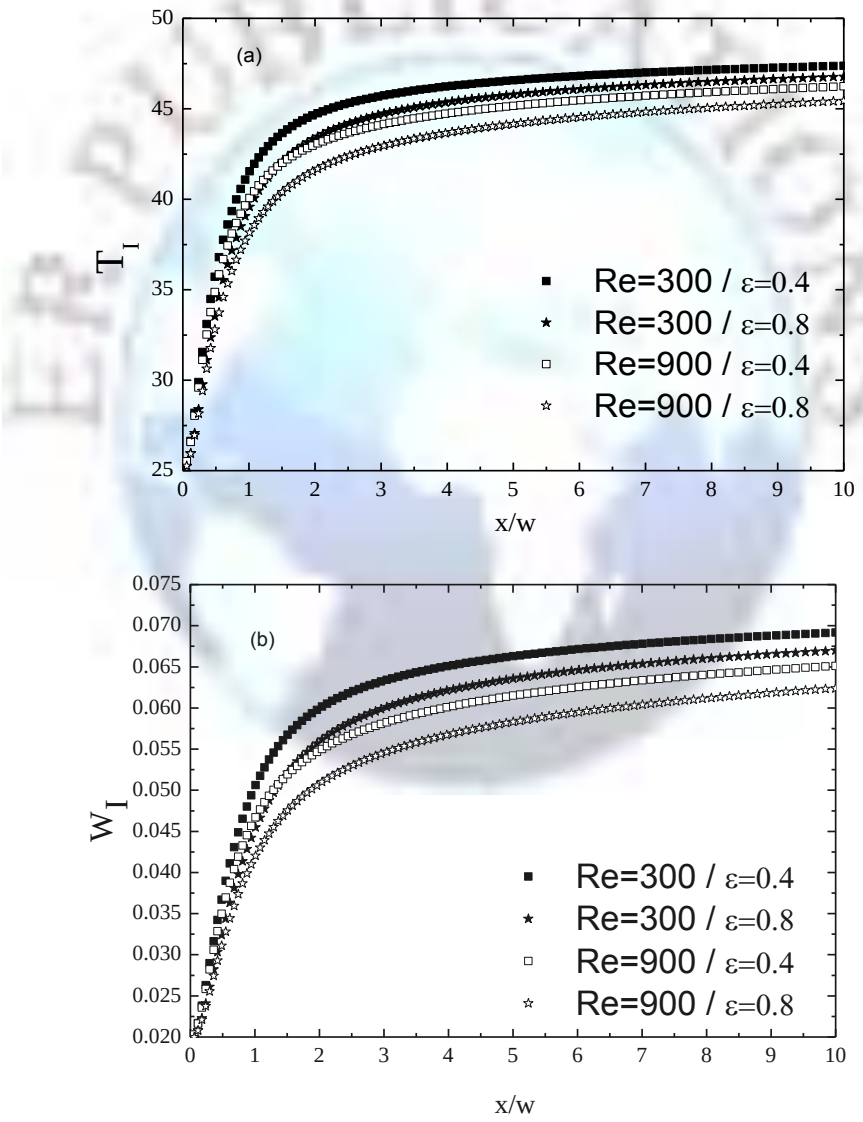

Figure 3. Effect of porosity and Reynolds number of porous layer on the axial distributions of interfacial temperature and mass fractionwith $T_0=T_{L0}=25°C$, $P_0=1atm$, Tw=50°C and W=0.05m

In the evaporation of the liquid film, the heat transfer is achieved both by mechanisms of sensible and latent heat transfer. This study evaluates the influence of the porous structures and gas Reynolds number of the two mechanisms of heat

transfer. Figs 4(a, b) presented the effect of porous structures on the sensible and latent heat transfer rate (Q_s/Q_tandQ_L/Q_t) for various porosity (0.4, 0.8) and Reynolds number (300, 900). This figures show that the latent heat transfer is more important in a way huge than the sensible heat transfer.

In fig 4a, the sensible heat flux (Q_s/Q_t) Decrease rapidly in the flow direction to x/w=20 after this abscissa tends toward a constant value, and It is seen that with a higher value of porosity and Reynolds number(Q_s/Q_t) is more important.This result can be explained by to fact that the gradient of temperature at the interface is more important for a higher value of porosity and Reynolds number.

Differently in the fig 4b the latent heat flux (Q_L/Q_t) increase rapidly in the flow direction to x/w=20 after this abscissa tends toward a constant value, and it is seen that with a lower value of porosity and Reynolds number (Qs/Qt) is more important. This is readily understood by realizing that a reduction in the Porosity and Reynold number causes greater film evaporation and hence a higher latent heat flux.

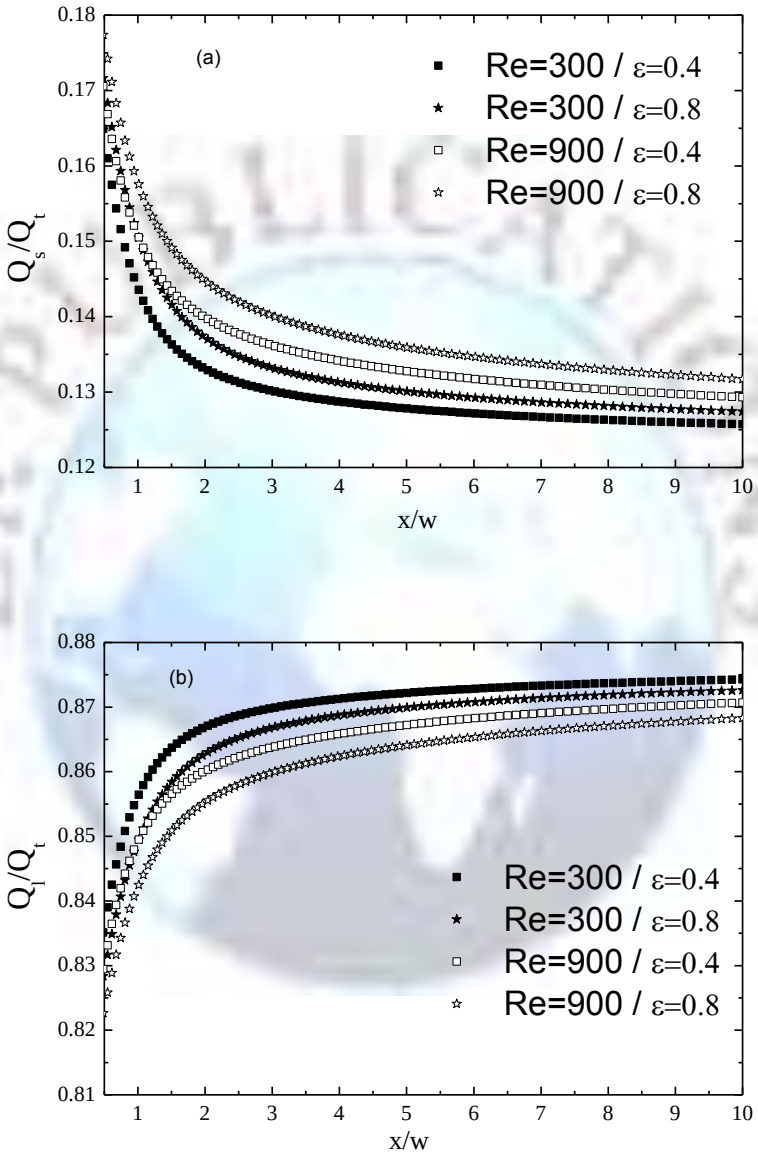

Figure 4. Effect of porosity and Reynolds number of porous layer on the axial distribution of sensible heat flux and latent heat flux with $T_0=T_{L0}=25°C$, $P_0=1atm$, Tw=50°C and W=0.05m

For more understanding the effect of porosity and Reynolds number the fig 5 illustrate the variations of dimensionless accumulated evaporation rates which increases towards the outlet channel. It's observed in this figure that the effect of Reynolds number is more important than the effect of porosity. In the other hand for a higher Reynolds number, greater liquid film vaporization is observed. Which implies that mass transfer is more effective in forced convection. This confirms the general concept that the larger evaporation will be obtained for forced convection.

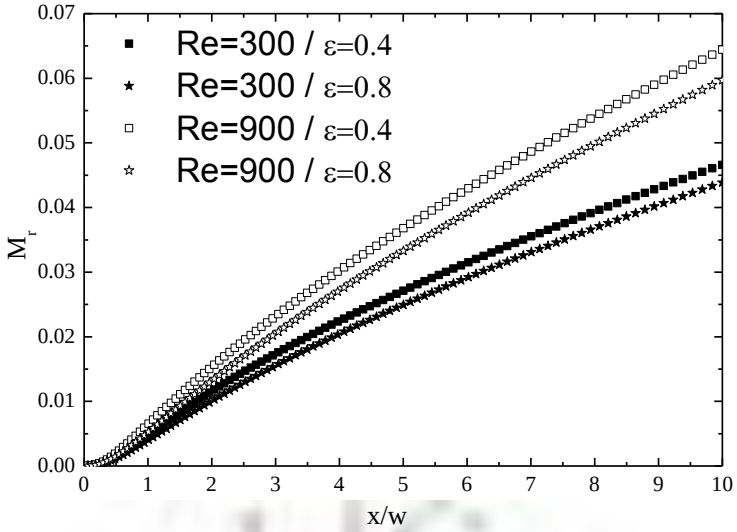

Figure 5. Effect of porosity and Reynolds number of porous layer on the axial distribution of the interfacial mass evaporation rate with $T_0=T_{L0}=25°C$, $P_0=1atm$, Tw=50°C and W=0.05m

D. Influence of Porosity and humidity

Figs 6(a, b) illustrates the effect of the porosity and air relative humidity on the interfacial temperature (a) and mass fraction (b). It is seen that the interfacial temperature and mass fraction increases rapidly at the entrance (x/w< 2) and then remains virtually constant along the axial direction. It's noted in this figure that the interfacial temperature increase as the porosity decrease or air relative humidity increase. Therefore, the corresponding mass fraction is larger for lower porosity or a larger air relative humidity. This can be explained by the fact that the porous layer increases the heat transfer of liquid film and hence, contributes in the effectiveness of heat transfer to the liquid film.

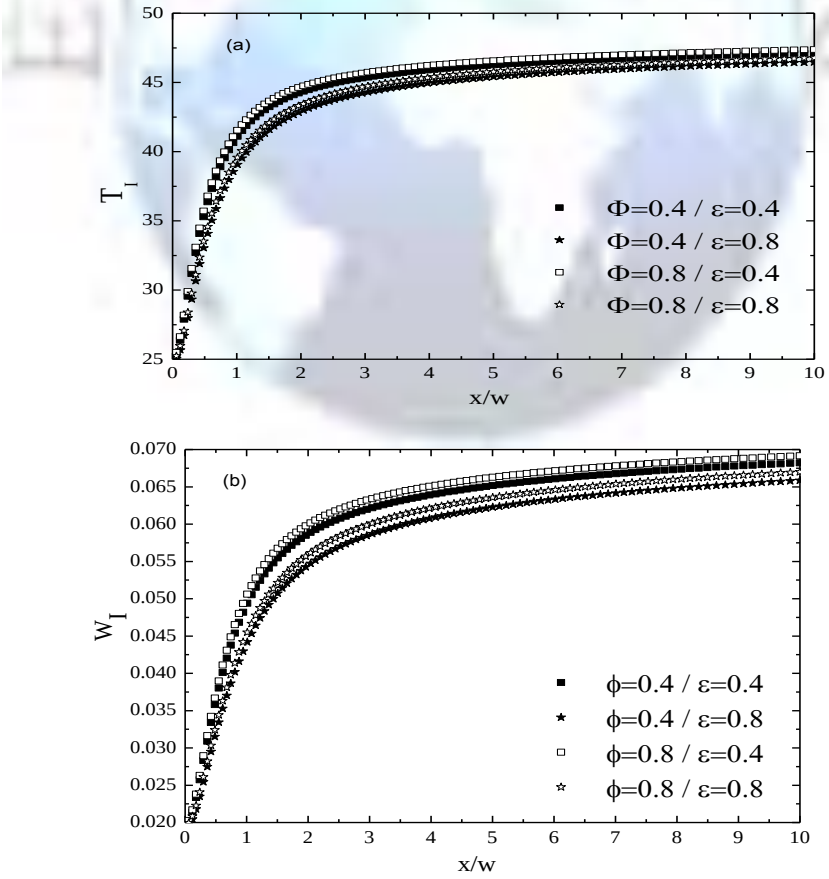

Figure 6. Effect of porosity and humdity of porous layer on the axial distributions of interfacial temperature and mass fraction with $T_0=T_{L0}=25°C$, $P_0=1atm$, Tw=50°C and W=0.05m

In liquid film evaporation, heat transfer is achieved by both sensible and latent heat transfer mechanisms. This both mechanism is depicts in figs 7 (a, b) with the influence of porous structures and humidity.

The analysis of the results of fig(a, b) shows that the sensible heat flux is more important with high value of porosity and humidity, but against the important value of the latent heat flux is obtained for lower value of the porosity and humidity. It's also observed that the effect of humidity is more important than the effect of porosity.

From inspection, it is found that latent heat exchange is about eight times larger than the sensible heat exchange and it is account for approximately 87% to 89% of the total heat transfer.

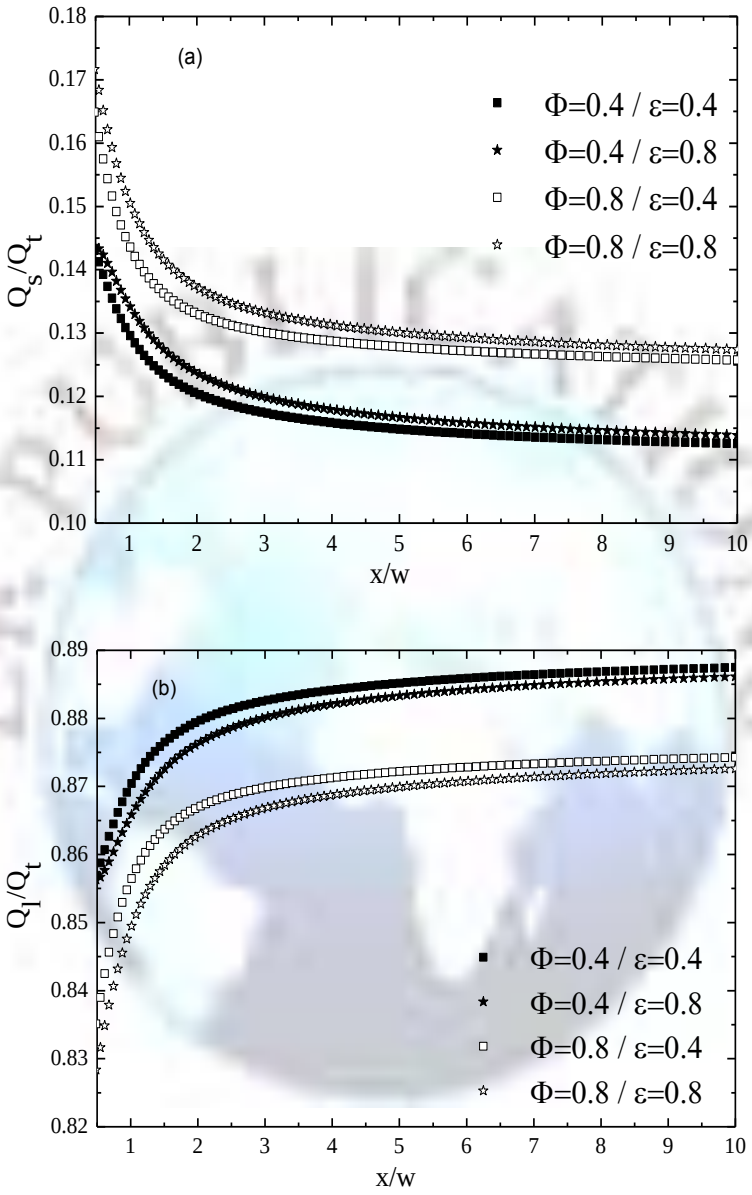

Figure 7. Effect of porosity and humidity of porous layer on the axial distribution of sensible heat flux and latent heat flux with $T_0=T_{L0}=25°C$, $P_0=1atm$, Tw=50°C and W=0.05m

Fig 8 illustrates the variations of interfacial mass evaporation rate with different values of porosity (ε= 0.4;0.8) and humidity (ϕ=0.4;0.8). As expected M_r increase with increasing x/w to the outlet channel.

It is apparent that interfacial mass evaporation rate is important for de lower values of porosity. This result can be justified by the fact that when we decrease of porosity, the conductivity of porous layer increase, which enhance the mass transfer process, and consequently an increase of interfacial mass evaporation rate. This implies that mass transfer is more effective in forced convection. In other hand we observed that a higher liquid mass evaporation rate increase from lower air relative humidity this is due to the tendency of air to absorbs more vapor as it was more drying.

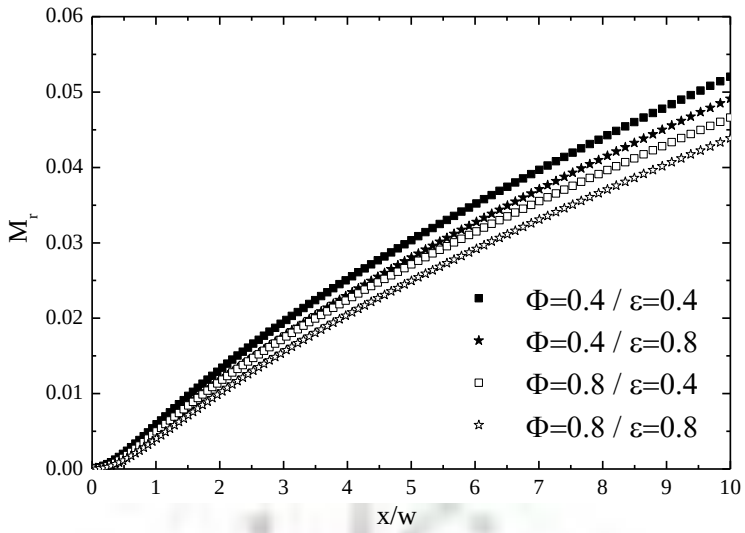

Figure 8. Effect of porosity and humidity of porous layer on the axial distribution of the interfacial mass evaporation rate with $T_0=T_{L0}=25°C$, $P_0=1atm$, Tw=50°C and W=0.05m

Conclusion

The characteristics of liquid film evaporation in forced convection flow in a porous medium were studied. The complete two dimensional laminar boundary layer models for the evaporating liquid andair flows along a vertical plate were adopted. The non-Darcian convective, boundary viscous, and inertia force effects are considered. Based on the numerical results obtained, the main conclusions from the study are summarized as follows:

We also observed that the latent heat transfer is still the dominant mode for the present study.

- Lower Reynolds number and porosity and higher humidity yield higher interfacial temperature and mass concentration, thus enhance the heat and mass transfer performances across the film interface.
- The magnitude of relative latent heat flux Q_L/Q_t,is much larger than the relative sensible heat flux Q_s/Q_t.This implies that transfer along the gas-liquid interface is dominated by latent heat transfer in conjunctionwith the liquid film evaporation.
- The influences of Reynolds number and humidity on the heat and mass transfer performance of liquid film evaporation are more important than the influences of porosity.
- Heat Mass transfers are enhanced for lower values of air humidity and porosity and higher Reynolds number.

References

[1]. M. Feddaoui, H. Meftah,A. Mir, "The numerical computation of the evaporative cooling of falling water film in turbulent mixed convection inside a vertical tube", Int. Comm Heat Mass Tran., Vol. 33, 2006, pp 917-927.

[2]. M. Feddaoui, A. Mir, " Turbulent mixed convection heat and mass exchanges in evaporating liquid film along a vertical tube". Int. J. Heat Exchangers, Vol. 7, 2007. pp 15-30.

[3]. D.A.S Rees, K.Vafai," Darcy-Brinkman free convection from a heated horizontal surface", Numer. Heat Tran. Vol.35, 1999, pp 191-204.

[4]. B. Alazmi, K.Vafai," Analysis of fluid and heat transfer interfacial conditions between a porous medium and a fluid layer", Int. J. Heat Mass Tran. Vol.44, 2001, pp 1735-1749.

[5]. J.S. Leu,J.Y. Jang, Y. Chou, " Heat and mass transfer for liquid film evaporation along a vertical plate covered with a thin porous layer", Int. J. Heat Mass Tran. Vol. 49, 2006, pp1937–1945.

[6]. Y.Chou, R.J. Yang. " the evaporation of a saturated porous layer inside an inclined airflow channel", Int. J. Heat Fluid Flow. Vol. 28, 2007, pp 407–417.

[7]. J.S. Jin-Sheng Leu, J.Y Jang, Y. Chou."Convection heat and mass transfer along a vertical heated plate with film evaporation in a non-Darcian porous medium". International Journal of Heat and Mass Transfer vol. 52, 2009, pp 5447–5450.

[8]. Y. El Hammami, M. Feddaoui, S. Senhaji, T. Mediouni, A. Mir "Turbulent mixed convection heat and mass transfer of liquid film evaporation by a porous layer along an inclined channel". revue internationale d'héliotechnique n° 39, 2009, 44-49.

[9]. Y. El Hammami, M. Feddaoui, S. Senhaji, T. Mediouni, A. Mir " Étude numérique de la condensation en film par convection mixte a l'intérieur d'un canal a paroi poreuse". revue internationale d'héliotechnique n° 42, 2010, 18-24.

[10]. A. Halder, A.K. Datta. "Surface heat and mass transfer coefficients for multiphase porous media transport models with rapid evaporation". Food and Bioproducts Processing. Vol. 90, 2012, pp 475–490.

[11]. B. Taouti, L. Bernard, B. Benyoucef, V. Joseph, "superficial evaporation in forced convection of porous medium in transitory laminates regime". Energy Procedia. Vol.18, 2012,pp. 966-973.
[12]. E.R. Eckert, R. M. Drake, "Analysis of heat and mass transfer", McGraw-Hill, New York, 1972, p. 806.
[13]. A. G. Fedorov, R. Viskanta, A.A. Mohamad, "Turbulent heat and mass transfer in an asymmetrically heated, vertical parallel-plate channel", Int. J. Heat Fluid Flow. Vol.18, 1997, pp 307-315.
[14]. T. Fujii, Y. Kato, K. Mihara [1977], Expressions of transport and thermodynamic properties of air, stream and water, Sei San Ga Ken Kyu Jo, Report No. 66, Kyu Shu Dai Gaku, Kyu Shu, Japan. pp 81-95.
[15]. R.C. Reid, and T.K. Sherwood, [1984], The properties of gases and liquids, Mc Graw Hill, New York.
[16]. S. V. Patankar, [1980]. Numerical heat transfer and fluid flow. New York : Hemisphere/Mc Graw Hill.
[17]. G. D Raithby, G.E. Schneider, [1979]. Numerical solution of problems in incompressible fluid flow: treatment of the velocity-pressure coupling, Num. Heat Tran. Vol. 2, pp 417-4.
[18]. S. Ergun, Fluid flow through packed columns, Chem. Eng. Prog. 48 (1952) 89–94.